Coupling of Spin, Substrate, and Redox Equilibria in Cytochrome P450†

Stephen G. Sligar

ABSTRACT: Cytochrome P450, both in the presence and absence of substrate, is shown to be a mixture of high- and low-temperature spectral forms, with the suggestion that these two forms correspond to the $S = 1/2$ and $S = 5/2$ spin states of the heme iron. The equilibrium constants and thermodynamic parameters describing the spin transition have been quantitated using high-resolution optical spectroscopy and are in excellent agreement with high-temperature Mössbauer and electron paramagnetic resonance spectroscopy results. The spin-state equilibrium is shown to modulate both the substrate binding and the oxidation-reduction potential of the cytochrome. These three interacting equilibria are presented in terms of a general thermodynamic model of regulation which provides a clear and concise description of the multicomponent reaction scheme.

Cytochrome P450 (abbreviated cytochrome m, or m for monoxygenase[1]) is a component of the mixed function oxidase system found in abundance in the soil bacterium *Pseudomonas putida* where it metabolizes the natural substrate, camphor, via a hydroxylation reaction converting the monoterpene to the corresponding 5-exo alcohol (Hedegaard and Gunsalus, 1965). The bacterial cytochrome P450, in direct analogy with the adrenal steroid synthesizing systems and the liver detoxification schemes, utilizes pyridine nucleotide as a source of the two electron equivalents required to cleave atmospheric dioxygen, inserts one atom into the carbon chain of the substrate, and reduces the other to water. In the bacterial reaction cycle, a flavoprotein dehydrogenase acts on NADH and is subsequently oxidized by an iron-sulfur redoxin of the Fe_2S_2*Cys_4 variety. This latter component, termed putidaredoxin (*Pseudomonas putida* ferredoxin) in the microbial system and abbreviated PD, donates two electrons labeled e_1 and e_2, in sequential fashion to the cytochrome containing the oxygen and substrate binding centers. The present understanding is compatible with the sequential reaction scheme shown in Figure 1 (Gunsalus et al., 1974). Oxidized (ferric) cytochrome, m^o, undergoes rapid substrate binding ($m^o + S \leftrightarrow m^{os}$) and is followed in turn by the input of e_1, which induces a ferric-ferrous reduction of the heme iron ($m^{os} + e_1 \leftrightarrow m^{rs}$), and oxygen addition ($m^{rs} + O_2 \leftrightarrow m_{O_2}{}^{rs}$). The oxygenated intermediate then decays, with the input of e_2, by substrate hydroxylation. Both e_1 ($PD^r + m^{os} \leftrightarrow PD^o + m^{rs}$) and e_2 ($PD^r + m_{O_2}{}^{rs} \rightarrow PD^o + S\text{-}OH + H_2O + m^o$) are donated by putidaredoxin and have been shown to occur through stable PD-cytochrome complexes (Sligar, 1975a; Sligar and Gunsalus, 1976; Pederson et al., 1976). A complete molecular description of the hydroxylation cycle requires a precise understanding of these two electron-transfer reactions and their coupling with other equilibria in the camphor monoxygenase.

Substrate free P450, m^o, exists as a mixture of high, $m_{hs}{}^o$, and low, $m_{ls}{}^o$, spin states, being predominantly a low-spin ferric protein (total spin, $S = 1/2$) (Sharrock et al., 1973). The camphor bound form also exists as a mixture of spin states, $m_{hs}{}^{os}$ and $m_{ls}{}^{os}$, with substrate binding yielding a virtually complete high spin ($S = 5/2$) form (Tsai et al., 1970; Sharrock et al., 1973; Champion et al., 1975; Sharrock et al., 1976). Recent work has shown that the low-spin fraction of cytochrome is not homogeneous, but composed of at least two distinct forms (Lipscomb, 1974). Concomitant with the substrate induced change in electron spin state is an observable shift in the equilibrium redox potential of the cytochrome on binding of camphor (Sligar and Gunsalus, 1976). Thus, in the first two reactions of the cycle (Figure 1), three interacting equilibria are present: (1) substrate binding, (2) oxidation-reduction of the heme group, and (3) interconversion of the system between high and low spin states. Description of multicomponent interacting equilibria is best presented in terms of a free-energy diagram which graphically illustrates the coupling of the individual one-step reactions (Sligar and Gunsalus, 1976). In this publication, the interaction of spin, redox, and substrate equilibria will be examined in fundamental terms. Emerging will be not only a precise documentation of these processes in the camphor monoxygenase but also a basic insight into the general methods and mechanisms involved in the regulation and control of oxidation-reduction equilibria in cytochrome systems.

Materials and Methods

Cytochrome m was purified from *Pseudomonas putida* strain PpG 786 as previously described (Gunsalus et al., 1974). Extinction coefficients used in this study are those reported in that reference. Redox potentials were measured by the dye photoreduction method (Greenbaum et al., 1972; Sligar and Gunsalus, 1976). Absorption measurements were carried out using a Heath EU 707 spectrophotometer system interfaced on-line to a Wang 600 computer. This computer contains 3600 words of memory, direct access to the University's DEC-10 system via asynchronous ASCII lines, high-speed paper tape reader, and outputs on a Wang 602 plotting writer. Precise absorbance readings were obtained by digitizing the analogue signal with a Keithley Model 190 voltmeter (10^{-5} absorbance units resolution) and averaging 200 separate measurements taken at 0.5-s intervals. Temperatures were controlled to ±0.1 °C by a Haake FK-10 bath, with cuvette temperature monitored by Yellow Springs Instrument thermistors.

The Soret optical spectra of heme proteins have been shown to correlate with the spin state of the iron quantitated by con-

† From the Department of Biochemistry, University of Illinois, Urbana, Illinois 61801. *Received July 1, 1976.* This work was supported by National Institutes of Health Grants AM 00562 and GM 18051.

[1] Abbreviations used: NMR, nuclear magnetic resonance; EDTA, ethylenediaminetetraacetic acid; cytochrome P450 is abbreviated cytochrome m or m (Sligar et al., 1974), in order to simplify the labeling of redox, spin, and ligand states; NADH, reduced nicotinamide adenine dinucleotide; PD, putidaredoxin.

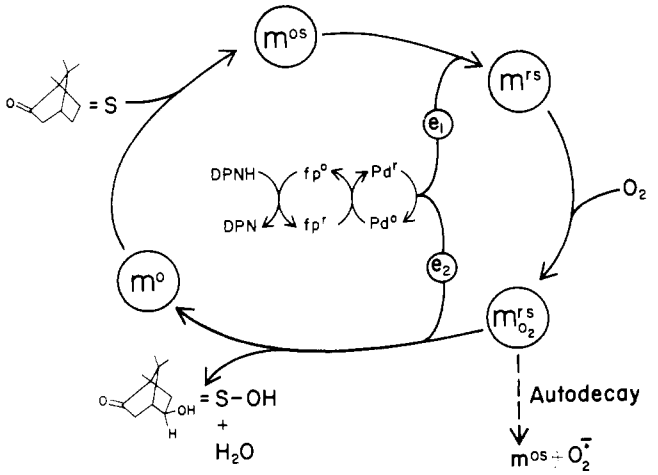

FIGURE 1: Cytochrome P450 reaction cycle. Cytochrome P450 is abbreviated m for monoxygenase (Sligar et al., 1974) in order to simplify labeling of ligand and redox states. The reactions indicated are sequentially: (1) camphor binding, $m^o + S \leftrightarrow m^{os}$; (2) ferric-ferrous reduction of the heme iron, $m^{os} + e_1 \leftrightarrow m^{rs}$; (3) oxygen addition, $m^{rs} + O_2 \leftrightarrow m_{O_2}^{rs}$; (4) input of e_2 and substrate hydroxylation. Both reducing equivalents, e_1 and e_2, originate from pyridine nucleotide (NADH or DPNH) and are supplied through a flavoprotein (fp) reductase and putidaredoxin (PD).

ventional magnetic resonance experiments (George et al., 1964; Beetlestone and George, 1964; Smith and Williams, 1968; Iizuka and Yonetani, 1970).

Thus we have chosen to follow the spin-state transitions in cytochrome P450 by the shift in the position of the Soret maxima, low-spin ferric protein being characterized by a maximum in the 417-nm region, while high spin is labeled by a blue-shifted maxima near 391 nm (Figure 2).

As will be discussed in a later section, comparison of spin state measured by optical spectroscopy with those obtained by nuclear magnetic resonance susceptibility and Mössbauer measurements is in excellent agreement. The monitoring of room-temperature variations by optical spectroscopy thus complements Mössbauer and electron paramagnetic resonance measurements as a tool for precise determination of equilibrium constants. If A_{hs} and A_{ls} represent respectively the absorbances at a given wavelength for pure high- and low-spin forms of the cytochrome, then the spin equilibrium constant for an absorbance A defined as a ratio of high- and low-spin concentrations is given by $K = [m_{hs}]/[m_{ls}] = (A - A_{ls})/(A_{hs} - A)$. The temperature-dependent spectra of m^o and m^{os} were analyzed by fitting the derived absorbance values to an Arrhenius relation using A_{hs} and A_{ls} as parameters and the standard correlation coefficient as a convergence parameter. Values of A_{hs} and A_{ls} so derived are compatible with the independently derived extinctions for m^{os} (predominately high spin) and m^o (predominately low spin).

All experiments were conducted in 50 mM potassium phosphate buffer, pH 7.0, containing 160 mM potassium chloride and 700 μM camphor. The potassium concentration is crucial and was kept rigidly constant, as the ionic strength drastically affects the redox potentials, spin equilibrium constants, and camphor binding (S. Philson and S. Sligar, unpublished results).

Temperature-jump measurements were performed on a Messanlagen SBA7 transient spectrometer. Anode current from the 1P28A phototube was converted to a voltage with a Harris 2065A amplifier and recorded on a Tektronix 7000 series storage oscilloscope with differential input amplifier.

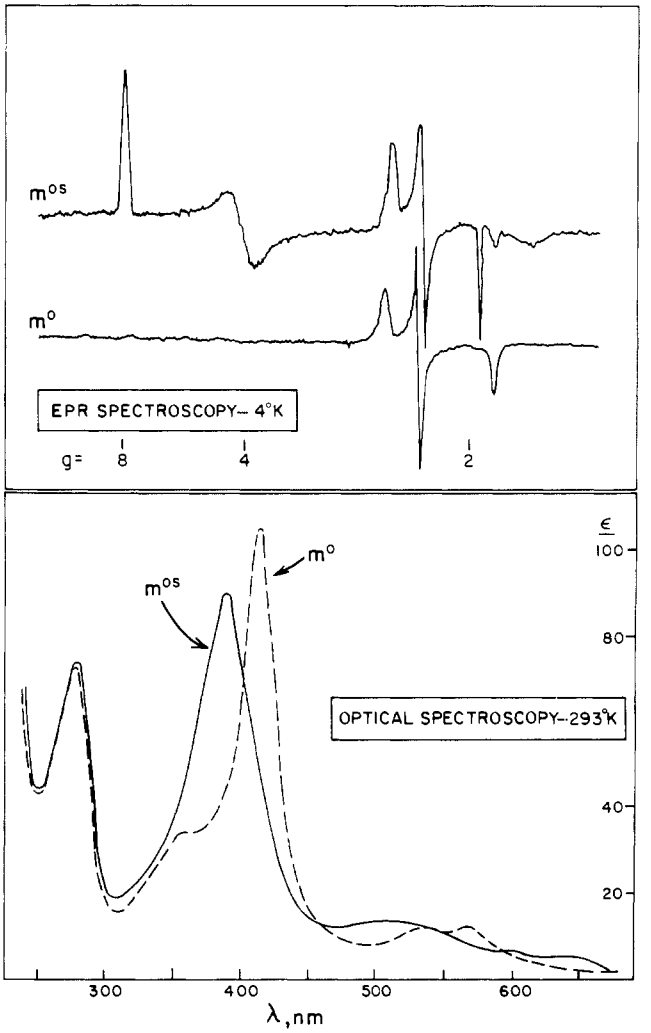

FIGURE 2: Substrate modulation of the cytochrome m spin state. The upper block shows electron paramagnetic resonance spectra at liquid helium temperature. m^o is seen to be a predominantly low-spin protein, while the substrate bound form is a mixture of spin states. Room temperature optical spectra reflect this difference between m^o and m^{os}. The almost complete high-spin m^{os} species is characeterized by a Soret maximum near 390 nm, as opposed to the low-spin substrate free protein, m^o, which has a maximum at 417 nm.

Results

The four states of ferric P450 (cytochrome m) representing the combinations of high–low spin and substrate binding are shown graphically in Figure 3. Each of the states is connected by the camphor binding ($m^o + S \leftrightarrow m^{os}$) spin ($m_{hs}^o \leftrightarrow m_{ls}^o$ or $m_{hs}^{os} \leftrightarrow m_{ls}^{os}$) reactions described by the equilibrium constants and free-energy changes defined below:

$$K_1 = [m_{hs}^o]/[m_{ls}^o] \quad (1)$$

$$K_2 = [m_{hs}^{os}]/[m_{ls}^{os}] \quad (2)$$

$$K_3 = [m_{ls}^o][S]/[m_{ls}^{os}] \quad (3)$$

$$K_4 = [m_{hs}^o][S]/[m_{hs}^{os}] \quad (4)$$

$$\Delta G_i = RT \ln K_i \qquad i = 1, \ldots, 4 \quad (5)$$

The four equilibrium states so described constitute a closed system with conservation of energy linking the individual steps:

$$\Delta G_1 + \Delta G_3 = \Delta G_2 + \Delta G_4$$

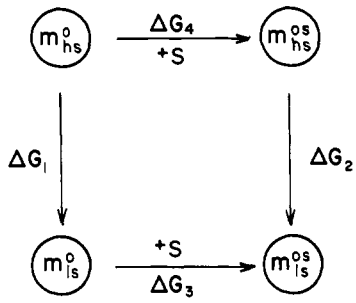

FIGURE 3: Ligand and spin states of ferric cytochrome m. One-step transition energies for the interacting equilibria are shown. Subscripts of hs and ls refer to high- and low-spin forms of the cytochrome, respectively. A superscript S indicates substrate bound.

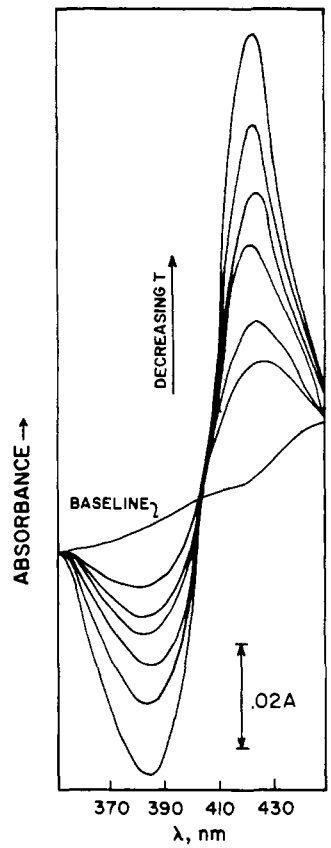

FIGURE 4: Temperature-induced difference spectra of cytochrome m^{o}. The substrate-free cytochrome is incubated at 27 °C in the reference compartment of a double-beam spectrophotometer, while the temperature of an identical aliquot in the sample compartment is varied. Increased displacements from the baseline correspond to 294, 291, 289, 285, 282, and 277 K. The indicated spectral differences are completely reproducible on cyclic temperature variation.

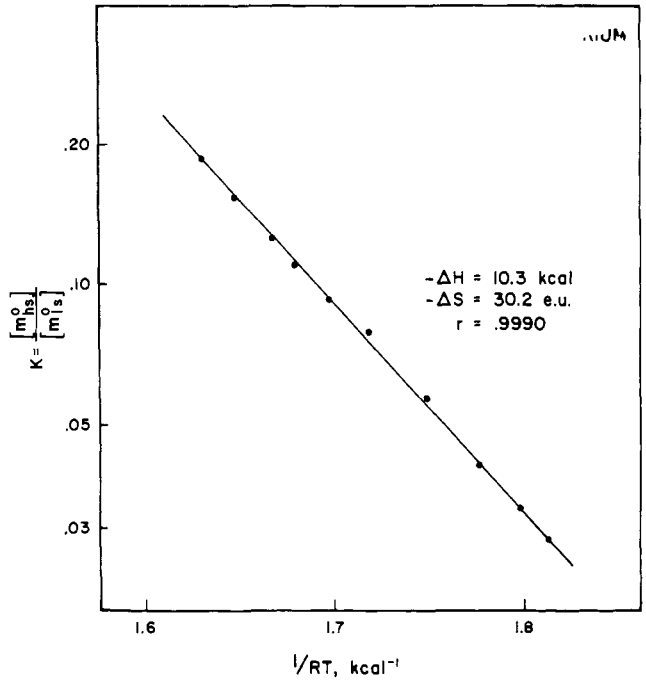

FIGURE 5: Equilibrium constant for the m^{o} spin equilibrium as a function of temperature. The temperature-induced difference spectra of m^{o} (Figure 4) were analyzed as described in Materials and Methods. Enthalpy and entropy values describing the process are shown. The correlation coefficient, r, is used as a convergence parameter in the fitting routine.

Using eq 5, this can be alternatively expressed as an obvious multiplicative relation among the equilibrium constants:

$$K_1K_3 = K_2K_4$$

A complete description of the interacting camphor binding and spin equilibria is thus realized by providing an independent measure of the constants K_1, K_2, K_3, and K_4. Quantitation of the spin equilibrium constants K_1 and K_2, in the absence and presence of the substrate camphor, will be described first.

Temperature-Dependent Difference Spectra of m^{o} and m^{os}. An optical difference spectrum of cytochrome m results when the reference cuvette is held at ambient temperature and the sample cuvette is regulated at varying temperatures from near freezing to in excess of 300 K. Figure 4 shows this experiment for the substrate free protein, m^{o}. When the resulting absorbance changes are fit to an equilibrium constant following an Arrhenius temperature dependence according to the procedure outlined in Materials and Methods, a linear van't Hoff plot results (Figure 5). The data are described by an overall enthalpy $\Delta H = -10.3$ kcal and entropy $\Delta S = -30.2$ eu corresponding to the reaction $m_{hs}^{o} \leftrightarrow m_{ls}^{o}$. These thermodynamic parameters yield an equilibrium constant $K_1 = [m_{hs}^{o}]/[m_{ls}^{o}]$ of 0.084 at 20 °C, illustrating the small concentration of high-spin material in the substrate-free case. When the same temperature variation is carried out with completely camphor saturated cytochrome (Figure 6), again an increase in the low-spin fraction is observed with decreasing temperature. A similar analysis (Figure 7) yields thermodynamic parameters of $\Delta H = -2.47$ kcal and $\Delta S = -13.8$ eu corresponding to an equilibrium constant $K_2 = [m_{hs}^{os}]/[m_{ls}^{os}] = 15$ at 20 °C. These values are summarized in Table I, together with the total free energies represented by the equilibria calculated from the relation $\Delta G = RT \ln K$. The concluding section will deal with a discussion of these thermodynamic parameters, but first the binding of substrate to the cytochrome in both spin states must be quantitated.

Substrate Binding to Cytochrome m. The binding of substrate to cytochrome m can be graphically represented as a four-state system with one-step equilibria depicted in Figure 3 and the insert to Figure 8. The free energies contained in the m^{o} and m^{os} spin equilibria have been defined by the temperature-dependent difference spectra described in the preceding section. All that remains for a complete energetic picture of the interaction between spin and substrate binding to ferrous cytochrome is to quantitate the camphor association to high- and low-spin forms. As observed initially, camphor binding shifts the spin equilibrium to the $S = \frac{5}{2}$ form and, hence, it must follow from energy conservation (Sligar and Gunsalus,

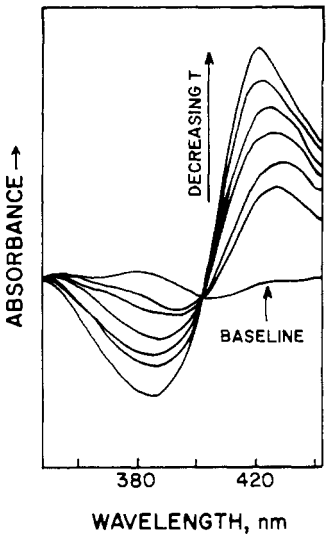

FIGURE 6: Temperature-induced difference spectra of cytochrome m^{os}. Substrate-bound cytochrome was used in an experiment analogous to that described in the legend to Figure 4. In this case, the reference temperature was 25 °C with the sample varied from 277 to 295 K.

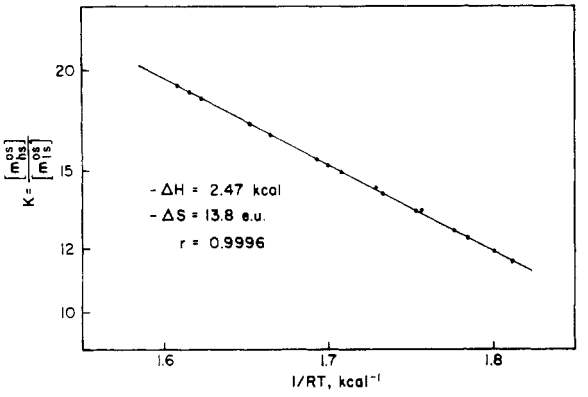

FIGURE 7: Equilibrium constant for the m^{os} spin equilibrium as a function of temperature. Conditions are described in Materials and Methods and the legend to Figure 5, using in this case, the substrate-bound cytochrome.

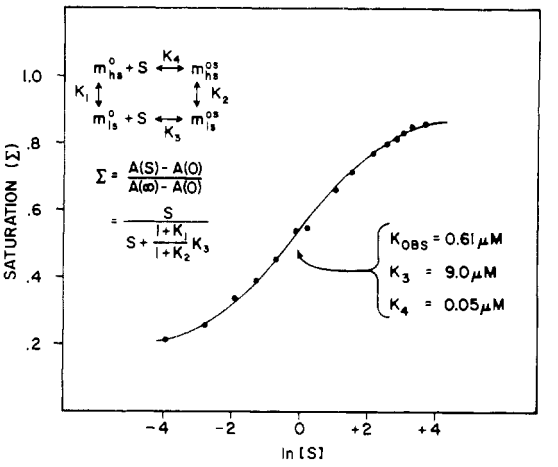

FIGURE 8: Substrate binding to ferric cytochrome m. Camphor binding to the high- and low-spin forms of oxidized protein in the scheme shown in the upper left corner. The saturation, $\sum$, follows a standard titration curve with the observed dissociation K_{obsd} being a function of the microscopic parameters K_1, K_2, K_3, and K_4. Free-energy conservations provide the equality $K_1K_3 = K_2K_4$. See text.

TABLE I: Thermodynamic Parameters of the Cytochrome m Spin Equilibrium.[a]

	Parameter	$-\Delta S$ (eu)	$-\Delta H$ (kcal/mol)	ΔG (kcal/mol)	K (20 °C)
$m_{ls}^{o} \leftrightarrow m_{hs}^{o}$	K_1	30.2	10.3	−1.44	0.084
$m_{ls}^{os} \leftrightarrow m_{hs}^{os}$	K_2	13.8	2.5	+1.59	15

[a] $K = [m_{hs}]/[m_{ls}] = \exp[-\Delta S/R + \Delta H/RT]$.

TABLE II: Substrate Binding to Cytochrome m.

	Parameter	K_D (μM)	ΔG (kcal/mol)	Method of Calculation
$m^{o} + S \leftrightarrow m^{os}$	K_a	0.61	−8.4	Obsd
$m_{ls}^{o} + S \leftrightarrow m_{ls}^{os}$	K_3	9.0	−6.8	$K_3 = K_a(1 + K_2)/(1 + K_1)$
$m_{hs}^{o} + S \leftrightarrow m_{hs}^{os}$	K_4	0.05	−9.8	$K_4 = K_3K_1/K_2$

1976) that substrate must preferentially associate to the high-spin state.

Camphor binding in the four-state model of cytochrome m (Figure 8) can be easily shown to follow simple stoichiometry. If $\epsilon(m_{hs}^{o})$ and $\epsilon(m_{ls}^{o})$ are the millimolar extinction coefficients for the high- and low-spin forms of substrate-free P450 with $\epsilon(m_{hs}^{os})$ and $\epsilon(m_{ls}^{os})$ being those corresponding to the substrate bound form, then the observed absorption A_S at any ligand concentration is:

$$A_S = \epsilon(m_{hs}^{o})[m_{hs}^{o}] + \epsilon(m_{ls}^{o})[m_{ls}^{o}] + \epsilon(m_{hs}^{os})[m_{hs}^{os}] + \epsilon(m_{ls}^{os})[m_{ls}^{os}]$$

The observed saturation, $\sum$, is then

$$\sum = \frac{A_S - A_0}{A_\infty - A_0} = \frac{[S]}{[S] + K_3(1 + K_1)/(1 + K_2)} \quad (6)$$

where K_3 is the dissociation constant for camphor binding to the low-spin form (eq 3) and [S] is the concentration of free camphor. A_0 is the initial absorbance with no substrate added and A_∞ the limiting value corresponding to complete saturation. Thus, the spectral titration of camphor binding follows standard functional form with an observed dissociation constant $K_{obsd} = K_3(1 + K_1)/(1 + K_2)$. It is important to note that $\sum$ represents the fraction of camphor bound, not the fraction high spin, and, thus, the above analysis is equally applicable to an equilibrium dialysis measurement of substrate binding. Figure 8 shows a standard analysis of the binding experiment, plotting the log of free camphor concentration as a function of the saturation $\sum$. The data follow the predicted functional form with an observed dissociation constant $K_{obsd} = 0.61$ μM. Together with the values of K_1 and K_2 obtained from the temperature-induced difference spectra, the above equations can be used to calculate a dissociation constant for binding to m_{ls}^{o}, K_3 of 9.0 μM (Table II). Conservation of energy $\Delta G_1 + \Delta G_3 = \Delta G_2 + \Delta G_4$, expressed alternatively as a product of equilibrium constants, $K_1K_3 = K_2K_4$, yield $K_4 = 0.05$ μM. The shift to high spin upon substrate binding is thus due to a 200-fold tighter association of camphor to this form.

The equilibrium constants describing the spin state, K_1 and K_2, together with the dissociation constants for camphor binding, K_3 and K_4, may be converted to standard free-energy changes, and used to construct a free-energy diagram describing the modulation of spin state by substrate binding.

TABLE III: Observable Lumped Parameters of Cube Model.

Reaction	Equilibrium Constant	Energy Equality
$m^o + S \leftrightarrow m^{os}$	$K_a = \frac{[m_{hs}^o] + [m_{ls}^o]}{[m_{hs}^{os}] + [m_{ls}^{os}]}[S] = \frac{1 + K_1}{1 + K_2} K_3$	$K_1K_3 = K_2K_4$
$m^r + S \leftrightarrow m^{rs}$	$K_b = \frac{[m_{hs}^r] + [m_{ls}^r]}{[m_{hs}^{rs}] + [m_{ls}^{rs}]}[S] = \frac{1 + K_9}{1 + K_5} K_8$	$K_8K_9 = K_5K_{12}$
$m^{os} + e^- \leftrightarrow m^{rs}$	$K_c = \frac{[m_{hs}^{os}] + [m_{ls}^{os}]}{[m_{hs}^{rs}] + [m_{ls}^{rs}]} = \frac{1 + K_2}{1 + K_5} K_7$	$K_2K_7 = K_5K_6$
$m^o + e^- \leftrightarrow m^r$	$K_d = \frac{[m_{hs}^o] + [m_{ls}^o]}{[m_{hs}^r] + [m_{ls}^r]} = \frac{1 + K_1}{1 + K_9} K_{10}$	$K_1K_{10} = K_9K_{11}$

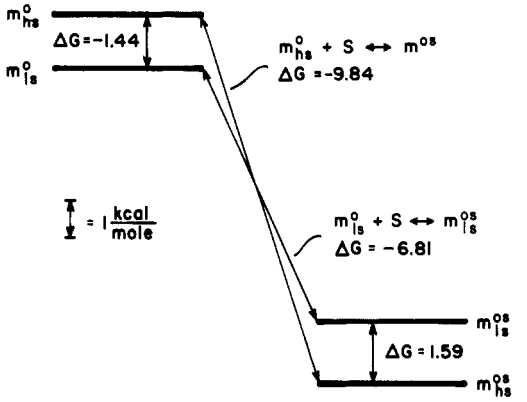

FIGURE 9: Substrate modulation of the cytochrome m spin equilibrium. An energetic picture of the regulation in the heme spin equilibria by substrate association is shown. All equilibrium constants have been converted to free-energy changes (in kcal/mol) via the relation $\Delta G = RT \ln K$.

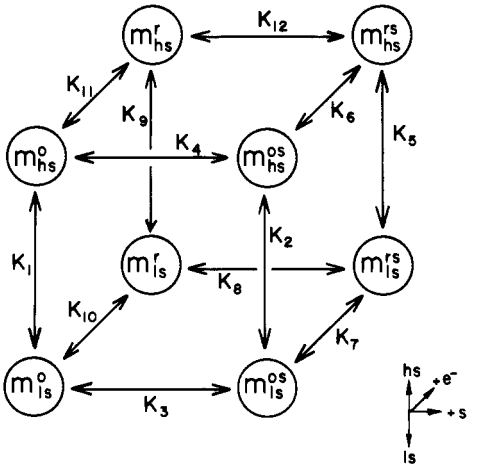

FIGURE 10: Redox, spin, and ligation states of cytochrome m. The four states of ferric protein (Figure 3) are extended to a third dimension by including those corresponding to the reduced cytochrome. The resulting cube structure has the equilibrium states connected by one-step transitions defined by the constants shown. (See text and Table III for further discussion.)

Figure 9 is a scale drawing graphically illustrating these points. It is clearly seen that the asymmetric binding of substrate to the high- and low-spin forms of the cytochrome is responsible for a lowering of the $S = 5/2$ energy level and a shift in the equilibrium to favor this state.

Spin and Substrate Modulation of the Cytochrome Redox Potential. The four states of spin and ligand reactions (Figure 3) are extended to a third dimension by inclusion of the corresponding ferrous forms resulting from the one electron reduction of cytochrome m. The resultant eight states can be represented by a cube structure (Figure 10) with the equilibrium constants describing the one-step transitions defined as shown. A complete thermodynamic picture consisting of a determination of each of these constants would emerge by duplicating the analysis described in the previous two sections using the ferrous protein. Measurement of the oxidation–reduction equilibria connecting the oxidized and reduced manifolds would then complete the equilibrium description. However, according to low temperature Mössbauer, and room temperature optical and NMR spectroscopy, ferrous P450 either with, m^{rs}, or without, m^r, substrate bound is in a virtually complete high spin ($S = 2$) configuration (Sharrock et al., 1976; Champion et al., 1975). It is thus at this time impossible to precisely quantitate the spin equilibria of ferrous cytochrome. An energy level corresponding to low spin ($S = 0$) material certainly exists, but is a great distance from the $S = 2$ ground state and hence is not populated under our observation conditions. With this limitation, an independent measurement of all the 12 equilibria represented by the cube edges in Figure 10 is impossible, although important conclusions can be drawn from those equilibria accessible to quantitation. This may be seen more clearly as follows. The 12 equilibria shown in Figure 10 are not all independent, being connected by conservation of energy and microreversibility conditions around all possible closed paths of the cube. Wyman has examined the topological constraints of this diagram and showed that, for a system with eight forms in three dimensions, there are only seven independent equilibrium constants (Wyman, 1976). We must thus ask how many independent parameters are amenable to measurement. Table III summarizes the four observables representing groupings of the fundamental equilibrium constraints. These relate to the observed dissociation values for substrate binding to the oxidized and reduced cytochrome, and the redox potentials (and hence equilibrium constants) connecting m^o and m^{os} to the ferrous states. These correspond to measurements dealing with the vertical faces of the structure shown in Figure 10. The equalities resulting from energy conservation around each of these vertical faces are also summarized in Table III. In addition to these four parameters, the individual spin equilibrium constants K_1 and K_2 have been determined. Without an independent determination of one of the ferrous spin equilibrium constants, therefore, only six parameters are available for independent quantitation and all microscopic free-energy changes contained in Figure 10 cannot be unambiguously determined.

The binding of substrate to ferrous cytochrome has been determined which corresponds to the equilibrium constant K_b (Griffin and Peterson, 1972). The redox potentials for substrate bound ($m^{os} \leftrightarrow m^{rs}$), ΔE_c, and free ($m^o \leftrightarrow m^r$), ΔE_d, cytochrome have also been quantitated (Sligar and Gunsalus,

TABLE IV: Substrate and Redox Equilibrium Constants.[a]

Reaction	Equilibrium Constant	Value[a]
$m^{o} + S \leftrightarrow m^{os}$	K_a	6.1×10^{-7}
$m^{r} + S \leftrightarrow m^{rs}$	K_b	4.5×10^{-9} [b]
$m^{os} + e^{-} \leftrightarrow m^{rs}$	K_c	8.0×10^{2}
$m^{o} + e^{-} \leftrightarrow m^{r}$	K_d	1.2×10^{5}

[a] At a temperature of 25 °C. [b] Griffin and Peterson (1972).

1976) as described in Materials and Methods, and can be converted to equilibrium constants (K_c and K_d, respectively) by the relation $K = \exp(-F\Delta E/RT)$, where the arbitrary reference potential is chosen as zero. These resulting equilibrium constants are summarized in Table IV. It can be easily shown by manipulating the various energy equalities that K_a, K_b, K_c, and K_d must satisfy (Sligar and Gunsalus, 1976):

$$K_a K_c = K_b K_d$$

This condition is met well within experimental error.

To further dissect the energetic analysis of the cube structure, an approximation must be made. As in all techniques explored, the ferrous proteins m^r and m^{rs} appear to be in a completely high spin ($S = 2$) configuration; $K_5 = [m_{hs}{}^{rs}]/[m_{ls}{}^{rs}]$ and $K_9 = [m_{hs}{}^{r}]/[m_{ls}{}^{r}]$ are much larger than unity. In analogy with eq 6, the measured dissociation constant for camphor binding to m^r is given by:

$$K_b = \frac{1 + K_9}{1 + K_5} K_8$$

or using the conservation of energy relation $K_8K_9 = K_5K_{12}$ by:

$$K_b = \frac{1 + K_9}{K_9} \frac{K_5}{1 + K_5} K_{12}$$

Hence for $K_9 \gg 1$ and $K_5 \gg 1$, $K_b = K_{12}$, and the observed dissociation constant for substrate binding to ferrous cytochrome m becomes equivalent to that for binding to the high-spin fraction. With this caveat, the binding of substrate to the high-spin protein in the ferric and ferrous state may be compared and will be discussed in the concluding section.

Temperature Jump Relaxation of the Cytochrome in Spin Equilibrium. Returning to the ferric cytochrome, in order to further probe the spin transitions of m^o and m^{os}, the $m_{hs}{}^{o} \leftrightarrow m_{ls}{}^{o}$ and $m_{hs}{}^{os} \leftrightarrow m_{ls}{}^{os}$ equilibria were examined by temperature-jump relaxation methods. When m^{os} was equilibrated at temperatures between 283 and 313 K and subjected to a 5 K perturbation, the spectral change indicative of a spin-relaxation process was faster than the dead time of the instrument, $<5 \times 10^{-6}$ s. However, when substrate free material, m^o, was subjected to the rapid temperature perturbation, a very slow exponential relaxation was observed (Figure 11) with a rate constant $k_f + k_b$ of 58 s^{-1}. Using $K_1 = k_b/k_f = 0.084$, k_f and k_b are calculated to be 53.5 and 4.5 s^{-1}, respectively. Quantitation of the perturbation amplitudes for both m^o and m^{os} as a function of the initial temperature yielded enthalpy values in good agreement with that determined by equilibrium measurements. The drastic changes in the rate of spin relaxation, dependent on the presence or absence of substrate, further illustrates the fine control camphor exercises in the equilibrium and dynamic aspects of the heme spin transition.

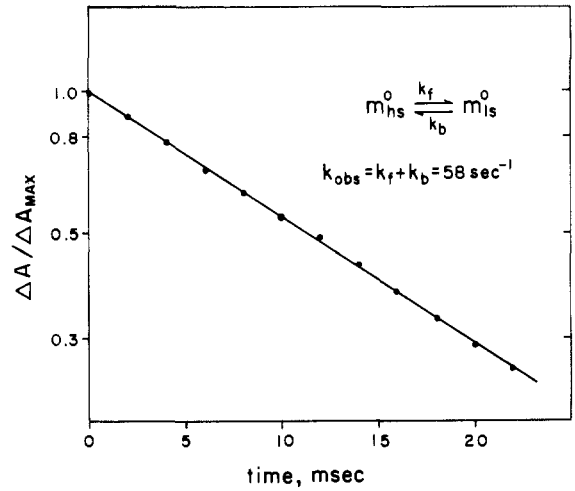

FIGURE 11: Temperature-jump-induced relaxation of the m^o spin equilibrium. m^o (15 μM) was perturbed by a 5 °C jump in temperature. The observed relaxation time of 12 ms is much longer than that observed for the substrate-bound cytochrome.

Discussion

Cytochrome m^o has been shown to exist as a mixture of high ($S = 5/2$) and low ($S = 1/2$) spin states. The equilibrium constant, K_1, for the reaction $m_{hs}{}^{o} \leftrightarrow m_{ls}{}^{o}$ has a value of 0.084 at room temperature which corresponds to $1/(1 + K_1) = 92\%$ of the protein being in the low-spin form. This equilibrium is drastically shifted on substrate binding, with the equilibrium constant, K_2, for the reaction $m_{hs}{}^{os} \leftrightarrow m_{ls}{}^{os}$ being 15, which corresponds to $K_2/(1 + K_2) = 94\%$ of the cytochrome existing in a high-spin configuration. These equilibrium constants were derived using high-resolution computer-averaged optical spectroscopy. It must be admitted that electronic spectra are not a priori a direct measure of the spin state of heme compounds. However, this technique was employed owing to the desire of quantitating these processes in the regions of room temperature and solution chemistry where comparisons with the previously measured and physiologically relevant redox potentials and ligation equilibria are applicable. In the case of m^{os} the parameters derived from the temperature-dependent optical spectra can be compared with those measured by the more conventional resonance techniques (Figure 12). The point at 200 K ($1/RT = 2.5$ $kcal^{-1}$) is from previous Mossbauer measurements (Sharrock et al., 1973). Although this value agrees well with the predictions based on optical spectra, at helium temperatures (~4 K) the Mossbauer and EPR spectra still show about 40% high-spin protein. The derived thermodynamic parameters, derived from optical measurements, however, predict a completely low-spin state. This difficulty at very low temperatures has not been resolved but could reflect a nonequilibrium distribution due to the cooling process or the possible appearance of other coupled reactions. Also included in Figure 12 is a single point at room temperature determined by S. Philson using NMR susceptibility techniques[2] (S. Philson and P. Debrunner, unpublished results). The excellent correlation with the optical result is strong indication that the observed perturbations in the electronic spectra are correlated

[2] This NMR susceptibility measurement was carried out with cytochrome m^{os} at 0.6 mM in 10 mM sodium phosphate buffer containing 20% ethylene glycol, 1 mM EDTA, 1 M potassium chloride, and 1.1 mM camphor.

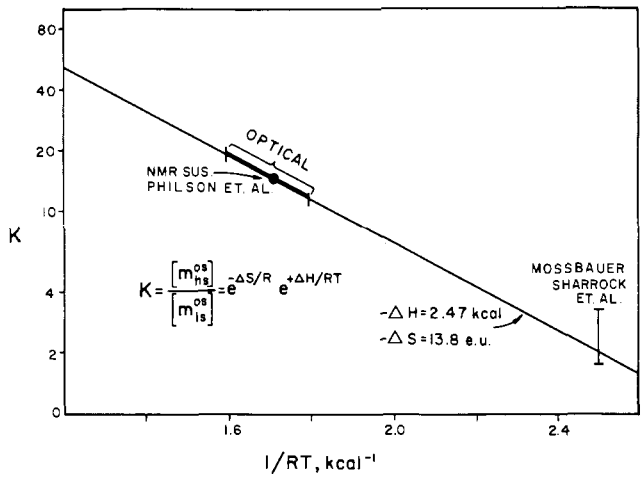

FIGURE 12: Comparison of m^{os} spin equilibrium quantitated by optical and resonance techniques. See Discussion and footnote 2.

with the spin state of the heme group. It should also be stressed that, in the temperature-induced spectral changes for both m^{o} and m^{os}, clean isosbestic points were observed with a clear shift in the position of the absorption maxima in the absolute tracings. These results tend to rule out the possibility of a simple temperature effect in the absorption line profile and justify the applicability of this technique to quantitation of the relevant equilibrium parameters.

From a theoretical standpoint, by considering only entropy contributions, a $S = \frac{1}{2}$ to $S = \frac{5}{2}$ transition between states with $2S + 1$ multiplicity is expected to contribute a ΔS on the order of R ln 3 or about 2 eu (see George et al., 1964, for a more detailed treatment). The much larger absolute entropy factors observed (14 eu for m^{os} and 30 eu for m^{o}) indicate the presence of other contributions in addition to a pure electron spin rearrangement. The central dogma (Williams, 1971) suggests that many high-spin heme compounds are formally five coordinated (the four pyrrole nitrogens of the porphyrin and a distal fifth ligand), while low-spin hemes are six coordinated. X-ray structures of model compounds and proteins (Perutz, 1970; Hoard, 1971) have shown that the ferric high-spin iron atom sits about 0.5 Å out of the porphyrin plane, while the low-spin iron is in-plane. Thus the steps involved in the high–low spin transition presumably also involve movement of the iron atom, alterations linked through the distal fifth ligand, as well as the binding of a sixth coordinating group. If the ligation at the proximal (sixth) position is by a weak solvent molecule a smaller change in the thermodynamic parameters might be involved than if the sixth coordinating group were a strong-field ligand that was an integral part of the globin structure. In this latter case, alterations could also be linked through movement of the liganding residue and its neighboring polypeptide chain. One might thus hypothesize that the spin transition in m^{o} involves the participation of an additional amino acid residue that coordinates in the transition of the heme to the $S = \frac{1}{2}$ state. The lesser magnitude of ΔH and ΔS for m^{os} could correspond to the participation of only a solvent molecule as the presumed obligatory proximal ligand inducing the low-spin form. These arguments are also consistent with the relaxation rates of the spin transition. The relaxation time for the reaction $m_{hs}{}^{os} \leftrightarrow m_{ls}{}^{os}$ is less than 5×10^{-6} s, while that for $m_{hs}{}^{o} \leftrightarrow m_{ls}{}^{o}$ is 12×10^{-3} s. Pure electron rearrangements would be expected to be very fast, $<10^{-7}$ s, and the involvement of solvent molecules introduces times on the order of the self-diffusion constant

TABLE V: Equilibrium and Relaxation Parameters of Heme Spin Equilibria.

Compound	$-\Delta H$ (kcal/mol)	$-\Delta S$ (eu)	k (s^{-1})
m^{os}	2.5	13.8	$>2 \times 10^{5}$
Metmyoglobin azide	3.7[a]	9.6[a]	$>5 \times 10^{5}$ [b]
m^{o}	10.3	30.2	58
Metmyoglobin imidazole	10.8[a]	32.7[a]	60[c]

[a] Iizuka and Yonetani (1970). [b] Beattie and West (1974). [c] Ligand exchange rate is bisimidazole *meso*-tetraphenylporphyrin (LaMar and Walker, 1972).

which are likewise very fast. The presence of an additional, possibly rate-limiting, ligation reaction, with perhaps concomitant movement of large moieties, however, is expected to be much slower.

The thermodynamic and kinetic parameters of the m^{o} and m^{os} spin equilibria summarized in Table I can be compared with similar values derived for other ferric heme proteins and model compounds. Table V documents the relaxation rates and enthalpy and entropy changes of these reactions for cytochrome P450, metmyoglobin hydroxide and metmyoglobin imidazole. The thermodynamic parameters of m^{os} are quite close to those measured for metmyoglobin azide (Iizuka and Yonetani, 1970) and metmyoglobin hydroxide (George et al., 1964). In all three protein species, the spin-relaxation rate is faster than the dead time of the temperature-jump instrumentation (Beattie and West, 1974). The thermodynamic parameters for the m^{o} spin transition, however, are more comparable to those for metmyoglobin with the strong field imidazole sixth ligand (Iizuka and Yonetani, 1970). In addition, there is surprisingly good agreement between the observed spin-relaxation rate for m^{o} and that for an imidazole exchange in the bisimidazole *meso*-tetraphenylporphyrin model compound (LaMar and Walker, 1972). These results could tentatively suggest that a histidine residue is involved in the $m_{hs}{}^{o} \rightarrow m_{ls}{}^{o}$ reaction, while only a solvent molecule participates in the corresponding transition with the substrate bound cytochrome. In addition, the loss of the proximal ligand on formation of the high-spin state in m^{o} would free this group for possible hydrogen bonding to the ketone group of the substrate. As a further hypothesis, such an additional factor could account for the increased affinity of the substrate for the high-spin form of the cytochrome. Diethyl pyrocarbonate modification of the histidine residues in cytochrome m (Lipscomb, 1974) yields a protein which is totally high spin and has lost its ability to revert to the low-spin configuration. This evidence, though admittedly tenuous, could further imply that an imidazole group is responsible for the low-spin transition in m^{o}. Laser temperature-jump measurements are in progress to quantitate the m^{os} spin relaxation and further elucidate the coupling between ligation and spin equilibria.

Turning to a discussion of reduced cytochrome (Table IV), the equilibrium constants for the reactions $m_{hs}{}^{o} \leftrightarrow m_{ls}{}^{o}$ (K_1) and $m_{hs}{}^{os} \leftrightarrow m_{ls}{}^{os}$ (K_2) allow calculation of the individual substrate binding parameters to the high- and low-spin forms (Figure 8 and Table II). The ferrous protein, on the other hand, both with or without substrate present, is in a virtually complete high-spin configuration, and thus $K_5 \gg 1$ and $K_9 \gg 1$. As was shown, under this approximation $K_b = K_4$ and the binding of camphor to reduced cytochrome represents the in-

herent association to the high-spin fraction. The values of K_4 and K_b can thus be compared in order to test the completeness of this analysis. From the experiments reported here, K_4 was calculated to be 0.05 ± 0.02 μM. Using pyridine competition with a P450 isolated from a different strain of *Pseudomonas putida* (Griffin and Peterson, 1972), K_b was measured as 0.005 μM. These values are actually close, considering their energetic distance from the corresponding low-spin state and the observed ferric dissociation constant. In addition, B. Shastry in this laboratory has completed synthesis of radioactive carbon and tritium labeled camphor. Equilibrium dialysis studies at 277 K yielded a dissociation constant of 0.05 μM (B. Shastry and I. C. Gunsalus, unpublished results), very close to that derived for binding to the high-spin fraction of cytochrome. It thus appears that, to a large extent, the spin state of the heme iron controls the association of camphor. Stated conversely, substrate binding to the cytochrome is predominantly a function of the spin and not oxidation state of the heme.

The oxidation–reduction potentials of m^o and m^{os} are also linked to the spin state. Since substrate binding is apparently affected only secondarily by the oxidation state, it follows from microreversibility that the redox potential of the cytochrome is not a strong function of the substrate binding reaction. Rather, these two equilibria are coupled through the modulation in the heme spin state. In this case, there corresponds for cytochrome m an inherent potential for reducing a pure high-spin and a pure low-spin protein. These are derived from the fundamental equilibrium constants K_6 and K_7, respectively (Figure 10). Note that if this is indeed the case, $K_6 = K_{11}$ and $K_7 = K_{10}$. As the agreement between K_6 and K_4 is not perfectly exact, substrate binding depends to some extent on the oxidation state of the heme, which in turn implies that camphor association is slightly active in modulating the redox potential. It is known that local hydrophobicity can drastically alter the oxidation–reduction equilibria of heme compounds (Kassner, 1973), and hence the presumed proximity of the nonpolar camphor skeleton in m^{os} could exert such an effect. Our presentation of the interacting equilibria in terms of the free-energy coupling model provides a definition of these two contributions and allows estimation of their relative importance. It should be noted that similar spin-state dependent changes in redox potential have been observed in the mitochondrial oxidative phosphorylation system (Wilson et al., 1972).

In summary, cytochrome m has been shown to exist as a mixture of high- and low-temperature spectral forms. Evidence is presented that these two species correspond to the heme states with total spin angular momentum of $S = \frac{1}{2}$ (low spin) and $S = \frac{5}{2}$ (high spin), with in all cases the lower temperatures favoring the low-spin configuration. Binding of the substrate camphor shifts the equilibrium to the $S = \frac{5}{2}$ state, as does reduction of the heme group to ferrous iron. The spin transition of substrate free cytochrome, m^o, is very slow by electronic standards and is characterized by large entropy and enthalpy changes. The camphor bound protein, m^{os}, relaxes at least 10^4 times faster with the equilibrium defined by correspondingly smaller thermodynamic parameters. These results suggest involvement of a strong-field ligand, such as an amino acid residue in the induced spin transition of m^o, but perhaps only a solvent molecule in m^{os}. The coupled spin, substrate, and redox equilibria are described in terms of a general thermodynamic model, with analysis showing that the spin state affects both camphor binding and oxidation–reduction reactions. Such a model may represent a general mechanism for regulation and control of cytochrome redox equilibria.

Acknowledgment

I express my sincere appreciation to Dr. I. C. Gunsalus for his support, consultation, advice, and friendship. The expert technical work of Ms. M. J. Namtvedt is gratefully acknowledged. I also thank T. Pederson, S. Philson, B. Shastry, L. Hanson, G. Wagner, P. Debrunner, and H. Frauenfelder for many valuable discussions. The editorial effort of Y. Lohse and N. Riddle was invaluable.

References

Beattie, J. K., and West, R. J. (1974), *J. Am. Chem. Soc. 96,* 1933.

Beetlestone, J., and George, P. (1964), *Biochemistry 3,* 707.

Champion, P. M., Lipscomb, J. D., Münck, E., Debrunner, P. G., and Gunsalus, I. C. (1975), *Biochemistry 14,* 4151.

George, P., Beetlestone, J., and Griffith, J. S. (1964), *Rev. Mod. Phys. 36,* 441.

Greenbaum, E., Austin, R., Frauenfelder, H., and Gunsalus, I. C. (1972), *Proc. Natl. Acad. Sci. U.S.A. 66,* 1157.

Griffin, B. W., and Peterson, J. A. (1972), *Biochemistry 11,* 4740.

Gunsalus, I. C., Meeks, J. R., Lipscomb, J. D., Debrunner, P. G., and Münck, E. (1974), in Molecular Mechanisms of Oxygen Activation, Hayaishi, O., Ed., New York, N.Y., Academic Press, p 559.

Hedegaard, J., and Gunsalus, I. C. (1965), *J. Biol. Chem. 240,* 4038.

Hoard, J. L. (1971), *Science 174,* 1295.

Iizuka, T., and Yonetani, T. (1970), *Adv. Biophys. 1,* 157.

Kassner, R. S. (1973), *J. Am. Chem. Soc. 95,* 2674.

LaMar, G., and Walker, F. (1972), *J. Am. Chem. Soc. 94,* 8607.

Lipscomb, J. D. (1974), Ph.D. Thesis, University of Illinois, Urbana, Ill.

Pederson, T. C., Austin, R. H., and Gunsalus, I. C. (1976), *Fed. Proc., Fed. Am. Soc. Exp. Biol. 35,* 1535.

Perutz, M. F. (1970), *Nature (London) 228,* 726.

Sharrock, M., Debrunner, P. G., Schulz, C., Lipscomb, J. D., Marshall, V., and Gunsalus, I. C. (1976), *Biochem. Biophys. Acta 420,* 8.

Sharrock, M., Münck, E., Debrunner, P. G., Marshall, V., Lipscomb, J. D., and Gunsalus, I. C. (1973), *Biochemistry 12,* 258.

Sligar, S. (1975a), Ph.D. Thesis, University of Illinois, Urbana, Ill.

Sligar, S., Debrunner, P. G., Lipscomb, J. D., Namtvedt, M. J., and Gunsalus, I. C. (1974), *Proc. Natl. Acad. Sci. U.S.A. 71,* 3906.

Sligar, S., Debrunner, P. G., Namtvedt, M. J., and Gunsalus, I. C. (1975b), *Fed. Proc., Fed. Am. Soc. Exp. Biol. 34,* 622.

Sligar, S., and Gunsalus, I. C. (1976), *Proc. Natl. Acad. Sci. U.S.A. 73,* 1078.

Smith, D. W., and Williams, R. J. P. (1968), *Biochem. J. 110,* 297.

Tsai, R., Yu, C. A., Gunsalus, I. C., Peisach, J., Blumberg, W., Orme-Johnson, W. H., and Beinert, H. (1970), *Proc. Natl. Acad. Sci. U.S.A. 66,* 1157.

Williams, R. J. P. (1971), *Cold Spring Harbor Symp. Quant. Biol. 36,* 53.

Wilson, D., Dutton, L., Erecinska, M., Lindsay, J., and Sato, N. (1972), *Acc. Chem. Res. 5,* 234.

Wyman, J. (1976), *Proc. Natl. Acad. Sci. U.S.A. 72,* 3983.